Biomechanical modelling of orthotic treatment of the scoliotic spine including a detailed representation of the brace–torso interface

D. Périé[1,2] C. E. Aubin[2,3] M. Lacroix[2,3] Y. Lafon[2,3]
H. Labelle[2]

[1]Department of Mechanical Engineering, University of Vermont, Burlington USA
[2]Research Center, Sainte-Justine Hospital, Montréal Canada
[3]Department of Mechanical Engineering, Ecole Polytechnique, Montréal Canada

Abstract—*As part of the development of new modelling tools for the simulation and design of brace treatment of scoliosis, a finite element model of a brace and its interface with the torso was proposed. The model was adapted to represent one scoliotic adolescent girl treated with a Boston brace. The 3D geometry was acquired using multiview radiographs. The model included the osseo-ligamentous structures, thoracic and abdominal soft tissues, brace foam and shell, and brace–torso interface. The simulations consisted of brace opening to include the patient's trunk followed by brace closing. To validate the model, the resulting geometry was compared with the real in-brace geometry, and the resulting contact reaction forces at the brace–torso interface were compared with the equivalent forces calculated from pressure measurements made on the in-brace patient. Differences between coronal equivalent and reaction forces were less than 7N. However, sagittal reaction forces (47N) were computed on the abdomen, whereas negligible equivalent forces were measured. The simulated geometry presented partially reduced coronal Cobb angles (1–4°), over-corrected sagittal Cobb angles and maximum deformation plane (5°), completely corrected coronal shift, and sagittal shift and rib humps that were not corrected. This study demonstrated the feasibility of a new approach that represents the load transfer from the brace to the spine more realistically than does the direct application of forces.*

Keywords—*Scoliosis, Finite element modelling, Boston brace, Brace–torso interface*

Med. Biol. Eng. Comput., 2004, **42**, 339–344

1 Introduction

THORACOLUMBOSACRAL ORTHOSIS is the most common non-surgical treatment in progressive adolescent idiopathic scoliosis. For instance, the Boston brace is an underarm orthosis made of polyethylene that is opened at the back and closed by two straps. By a combination of pressure points applied on the torso, it attempts to modify mechanically the scoliotic spine morphology and control the progression of spinal curvatures.

Numerical simulations of the orthotic treatment were generally made by applying forces representing brace pads to a model of the osseo-ligamentous structures of the torso. These models were used to study the brace mechanism in the correction of scoliosis. Traction forces were of relatively minor importance, compared with the lateral pads in the Milwaukee brace (ANDRIACCHI *et al.*, 1976). High thoracic pads reduced both thoracic and lumbar scoliotic curves more effectively than lumbar pads only in the Boston brace (PÉRIÉ *et al.*, 2003). Sub-axillary forces contributed, not only to the equilibrium of the trunk, but also to the correction of the curves in the Cheneau–Toulouse–Munster brace (PÉRIÉ *et al.*, 2002). These models also allowed investigation of optimised force configurations for the correction of scoliotic curves. A pad at the apex of the thoracic curve, without a counter pad, was proposed for thoracic curves, and a pad at the apex of the lumbar curve, with a thoracic counter pad, was proposed for lumbar curves (PATWARDAN *et al.*, 1986). Correction can be achieved in 3D with a combination of forces that reduce some adverse effects, such as flat back problems and limited axial rotation (GIGNAC *et al.*, 2000).

Little is known about the load transmission mechanism from the brace–torso interface to the spine. In the models including a representation of the rib cage (ANDRIACCHI *et al.*, 1976; AUBIN *et al.*, 1993; GIGNAC *et al.*, 2000; PÉRIÉ *et al.*, 2003; WYNARSKY and SCHULTZ, 1991), the load transmission from the skin to the ribs and the shear stresses were neglected, owing to the relatively

Correspondence should be addressed to Dr. Delphine Périé-Curnier; email: delphine.perie@online.fr

Paper received 28 May 2003 and in final form 27 January 2004
MBEC online number: 20043895

small thickness of the soft tissues. However, in the models without rib cage (PATWARDAN *et al.*, 1986; PÉRIÉ *et al.*, 2002) or in the lumbar area of all models, brace loads were applied directly on the vertebrae. The effective loads on the spine could be different from the real brace forces applied at the brace–torso interface and could affect the simulations. Other mechanisms than brace pads produce correction and contribute to the force equilibrium within the brace (PÉRIÉ *et al.*, 2003), such as muscles forces (ODERMATT *et al.*, 2003; WYNARSKY and SCHULTZ, 1991) or the righting reflex (OGILVIE, 1994). In the models that did not include the muscles, the applied forces were sometimes non-equilibrated and required restrictive boundary conditions, applied to the lower and upper parts of the spine, to fix the rigid translations and rotations. These restrictions entailed a stiffer behaviour of the whole spine and could also affect the simulations.

The aim of this study was to develop a detailed finite element (FE) model of the brace and its interface with the torso and a refined model of the trunk to simulate the Boston brace treatment. This detailed representation was developed to obtain a better transfer of the brace loads to the spine, compared with the simulations made by applying the brace forces directly to the ribs and spine.

2 Methods

The model was developed in a general manner, for any scoliotic patient, but, in this study, it was adapted to one adolescent girl (16.5 years old) with progressive idiopathic scoliosis (Cobb angles of 40° and 24°, respectively, for the thoracic and lumbar curves). She was treated by a Boston brace system. The experimental protocol comprised pressure acquisition at the brace–torso interface, followed by two radiographic acquisitions of the patient's torso geometry, the first one wearing the brace and the second one without the brace. Each of the two sets of radiographs was composed of a lateral (LAT) view, a standard postero-anterior (PA) view and a PA view with a 20° angled-down pitch. The subject positioning during the radiograph acquisition was controlled using a positioning apparatus that allowed patients to adopt a clinically relevant position, including specific positions of the hands, pelvis and feet. The entire protocol was performed on the same day at the brace delivery and was approved by the hospital ethics committee.

The personalised biomechanical model of the osseo-ligamentous structures of the trunk was previously reported (AUBIN *et al.*, 1995; DESCRIMES *et al.*, 1995; GIGNAC *et al.*, 2000) and is only summarised here. The geometrical data were obtained from anatomical landmarks, manually digitised on the radiographs, and reconstructed in 3D using the direct linear transformation (DLT) algorithm (Aubin *et al.*, 1995; GIGNAC *et al.*, 2000) and an atlas of already meshed generic vertebrae, which were deformed to fit the reconstructed points (AUBIN *et al.*, 1995). The accuracy of the multiview radiographic reconstruction technique is 3.3 ± 3.8 mm, and the variability is 0.8, 1.8, 5.3 and 7.5° for the PA thoracic, PA lumbar, LAT thoracic and LAT lumbar Cobb angles respectively, as presented by Delorme et al. (DELORME *et al.*, 2003). The vertebrae, intervertebral discs, ribs, sternum and cartilages were represented by 3D elastic beam elements, the vertebral and intercostal ligaments were represented by 3D elastic spring elements, and the costo-vertebral, costo-transverse and zygapophyseal joints were represented by surface-to-surface contacts, shell and/or multilinear elements (Table 1). Mechanical properties were taken from experimental and published data on cadaveric spines (DESCRIMES *et al.*, 1995).

The thoracic and abdominal soft tissues were represented by 1540 8-node brick elements supporting large deformations and presenting flexion capabilities (Fig. 1). The thoracic soft-tissue layer was extruded from the rib nodes and was 5 mm thick. This thickness, which influences the contact zones and forces but not the vertebral position results, was optimised for the computation of the contact reaction forces. A Young's modulus of 0.55 MPa and a Poisson coefficient of 0.45 were chosen from the literature (BISCHOFF *et al.*, 2000). The lumbar soft tissues were approximated as a cylinder that followed the sagittal spinal curve. The nodes from the 10th ribs were used to define the cylinder outline. The vertebral end-plate centres from L1 to L5 were used to define the curved axis of the cylinder. This cylinder was connected to the spine using the posterior nodes of the vertebrae and to the rib cage soft tissue using 8-node brick elements. The abdominal wall was represented by the elements located at the cylinder periphery, and the abdominal cavity was represented by the elements located at the cylinder centre. Young's moduli of 1 MPa and 0.01 MPa and Poisson coefficients of 0.2 and 0.45 were chosen from the literature (SUNDARAM and FENG, 1977;

Table 1 Element and mechanical properties used in model to represent patient's trunk, brace and brace–torso interface

	Element	Young's modulus, MPa	Poisson coefficient
Vertebral body	beams	1000	0.3
Pedicules	beams	5000	0.3
Apophysis	beams	35 000	0.3
Costo-vertebral, costo-transverse and zygapophyseal joints	multilinear springs + shells + surface-to-surface contacts	–	–
Intervertebral discs	beams	3.58–14.94	0.45
Ribs, bone	beams	5000	0.1
Sternum	beams	10 000	0.2
Ribs, cartilages	beams	480	0.1
Ligaments	3D elastic springs	1.49–6.49	–
Pelvis	beams	5000	0.2
Abdominal cavity	8-node bricks	0.01	0.45
Abdominal wall	8-node bricks	1	0.2
Thoracic soft tissue	8-node bricks	0.55	0.45
Brace–trunk interface	surface-to-surface contacts	–	–
Brace, rigid shell	8-node bricks	1000	0.2
Brace, foam	8-node bricks	100	0.45
Brace, straps	applied displacements	–	–

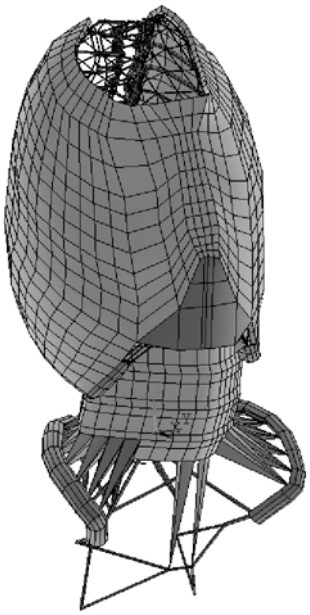

Fig. 1 *Refined finite element modelling of patient's trunk*

Fig. 2 *Flexible matrix composed of 192 pressure sensors*

UEYOSHI and SHIMA, 1985; DIETRICH et al., 1991; MARRAS and SOMMERICH, 1991) for the abdominal wall and cavity, respectively.

A personalised FE modelling of the brace was added to this trunk model. During the in-brace radiograph acquisition, a latex matrix (Fig. 2) containing 192 force-sensing transducers* was inserted at the brace–torso interface. The electric wires connecting the sensors could be visualised on the radiographs (Fig. 3*a*). They were reconstructed in 3D using the DLT algorithm (Fig. 3*b*). Two orthogonal sets of bicubic spline curves were used to interpolate the reconstructed points and to build quadratic surfaces. The brace, composed of a rigid shell and a foam layer, was represented by linear elastic 8-node brick elements created by external extrusions of the quadratic surfaces (Fig. 3*c*). Thicknesses of 3 mm and 4 mm, Young's moduli of 100 MPa and 1000 MPa, and Poisson coefficients of 0.45 and 0.2 were chosen for the foam and rigid shell, respectively, as specified by the manufacturer.

In the present study, we hypothesised that the brace was firmly fixed on the pelvis and had the same orientation as the pelvis. The comparison of the no-brace and in-brace acquisitions showed a rotation of the pelvis, as presented by LABELLE *et al.* (1996). Thus the brace model, built from the in-brace acquisition, was fitted on the no-brace patient's geometry using the rigid transformation of the pelvis from the in-brace to the no-brace acquisitions.

The brace–torso interface was represented by flexible surface-to-surface contact elements defined between the brace foam and the thoracic and abdominal soft tissues. These elements allowed status change when in contact, large deformation capability and sliding without friction.

The simulation of the Boston brace treatment was performed in two load steps. The first one consisted of the brace opening to include the patient's trunk, and the second one involved the brace closing (straps being fastned). Displacements allowing the brace to open and close were applied to the nodes located at the straps fixatings, symmetrically in the direction given by the strap fixating. As we measured the in-brace geometry using the electric wire of the in-brace acquisition, we obtained the final position of the straps fixating. Thus we opened the brace by applying an arbitrary 20 mm displacement to each strap insertion. Then, to avoid overloading, we closed the brace by applying the reverse displacement until the known final position. To avoid rigid displacements, a few nodes in the anterior region of the brace and on the patient's pelvis were space fixed. During the second step, the system state change was considered as the brace came in contact with the torso. The non-linearities due to the contact elements (status change) and to large deformations were taken into account, and both load-steps were solved using the Ansys 5.6 FE package†. A convergence tolerance factor for forces and displacements was chosen to reduce computation time without significantly influencing the vertebral position results.

The reaction forces recorded at the end of the simulation in the closed contact elements were compared with the equivalent forces calculated from the pressure measurements by means of localisation and magnitude (PETIT *et al.*, 1998). The accuracy of the pressure transducers was ± 5 mmHg, and the data collection was performed using the software (FSA 3.0) provided by the manufacturer of the pressure matrix. A clinically established pressure threshold of 30 mmHg (JIANG *et al.*, 1992) allowed pressure areas to be delimited in the thoracic, lumbar, pelvic and abdominal regions (right and left sides).

Total equivalent forces were calculated by discrete integration of pressure values on these areas using the Gauss method (MAC-THIONG *et al.*, 2004). The pressure sensors only allowed normal pressure to be measured and were not sensitive to shear forces. It was hypothesised that there were negligible shear and friction at the brace–torso interface. Thus the direction of these equivalent forces was aligned with the normal vector of the corresponding 3D pressure surface. The application node of these equivalent forces was determined using the minimum distance calculated between the nodes of the thorax and the pressure matrix surface using Voronoi polygons (Delaunay technique).

The simulated geometry of both the spine and rib cage was compared with the real, in brace geometry. The spine curves were analysed by means of vertebrae positions, angles between curvature inflexion points equivalent to the Cobb angle, in the PA and LAT planes, orientation of the maximum deformation plane, the PA and LAT shifts and transverse rib hump (DELORME *et al.*, 2003).

The influence of the brace model positioning on the results of the simulations was tested. To that end, various rigid transformations were used to position the brace on the no-brace patient's geometry: the rigid transformation of the pelvis from the in-brace to the no-brace acquisitions, the rigid transformation of L5 from the in-brace to the no-brace acquisitions, the rigid transformation of the S1/T1 axis from the in-brace to the no-brace acquisitions, and no transformation.

*Force Sensing Array, Verg, Winnipeg, Canada

†Ansys Inc., USA

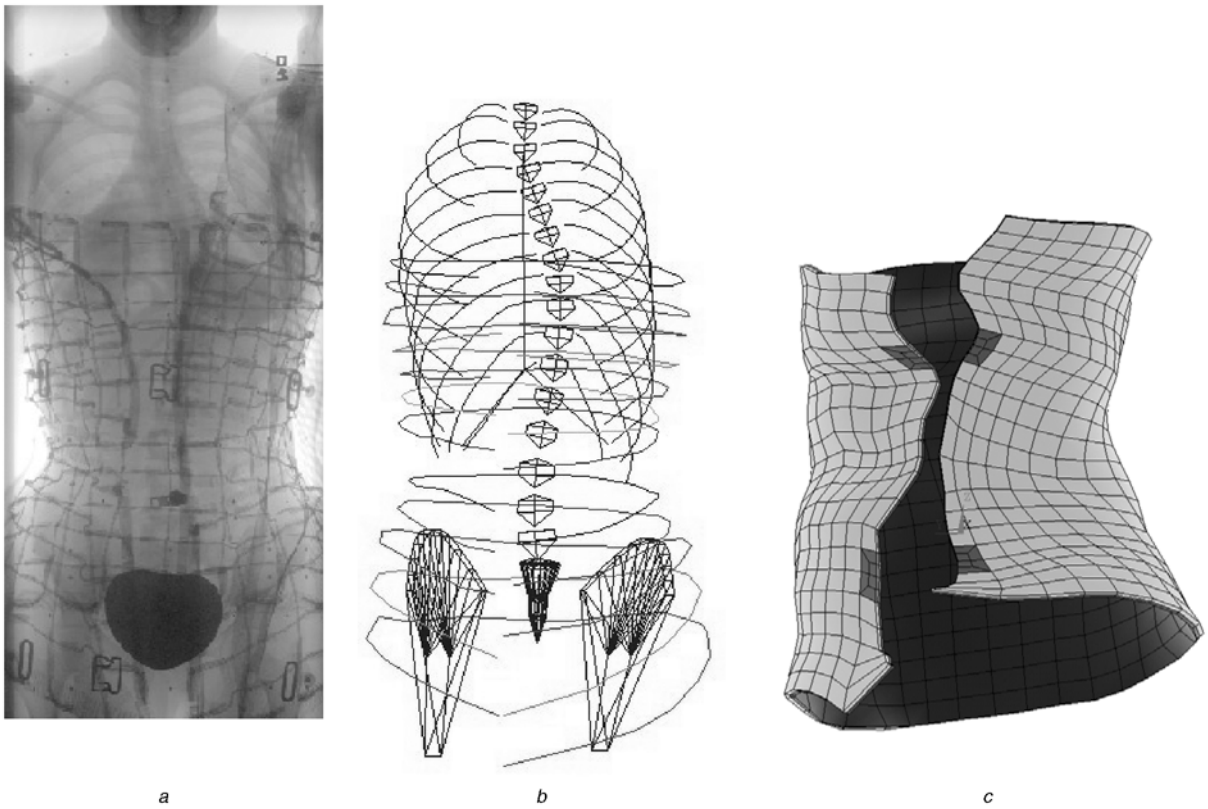

Fig. 3 *(a) Frontal radiograph of patient wearing Boston brace; (b) 3D reconstruction of electric wires, spine and rib cage; (c) finite element model of Boston brace*

3 Results

During the brace closure, right thoracic contacts appeared first, and the reaction forces shifted the spine away from them. Then, left contacts appeared, and the spinal curves were partially reduced.

Table 2 Equivalent forces from pressure measurements and contact reaction forces from simulation results. Global co-ordinate system was defined such that X-axis is sagittal axis pointing forward, Y-axis is coronal axis pointing to patient's left, and Z-axis is vertical axis pointing upwards (STOKES et al., 1994)

	Reaction forces (N)			Equivalent forces (N)		
Pad zone	*Fx*	*Fy*	*Fz*	*Fx*	*Fy*	*Fz*
Right lumbar	21	−20	−7	0	−17	0
Left lumbar	0	0	0	0	0	0
Right thoracic	−108	−79	−10	−37	−72	−38
Left thoracic	−9	16	−3	4	11	−3
Abdominal	47	−4	−11	0	0	0
Left sub-axillary	3	23	−3	0	0	0

Table 3 Geometrical parameters measured from no-brace and in-brace acquisitions and calculated from simulation results

	No brace	In brace	Simulation
Cobb PA thoracic, °	40	31	39
Cobb PA lumbar, °	−29	−16	−25
Cobb LAT thoracic, °	18	16	11
Cobb LAT lumbar, °	−33	−27	−22
Maximum deformation plane, °	49	15	9
Frontal shift, mm	−22	9	11
Sagittal shift, mm	−1	−7	−2
Transverse rib hump, °	−14	−7	−14

The closed contact elements presented reaction forces less than 7N different from the equivalent forces calculated from the pressure measurements in the coronal plane, for the lumbar and thoracic zones (Table 2). However, a sub-axillary force was calculated from the model (23N), but not from the pressure measurements. In the sagittal plane, higher reaction forces were computed from the model than from the pressure measurements.

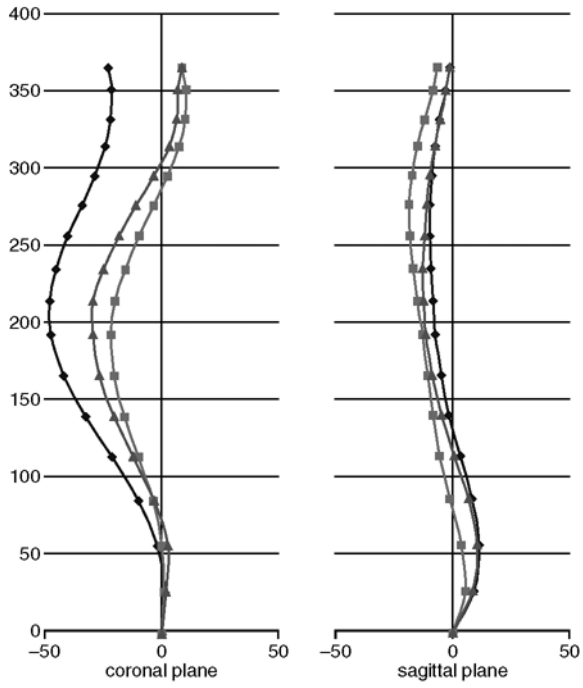

Fig. 4 *Spine curves of subject obtained from radiographic acquisitions (–■–) with and (–♦–) without brace and (–▲–) computed from FE model. All data are in mm*

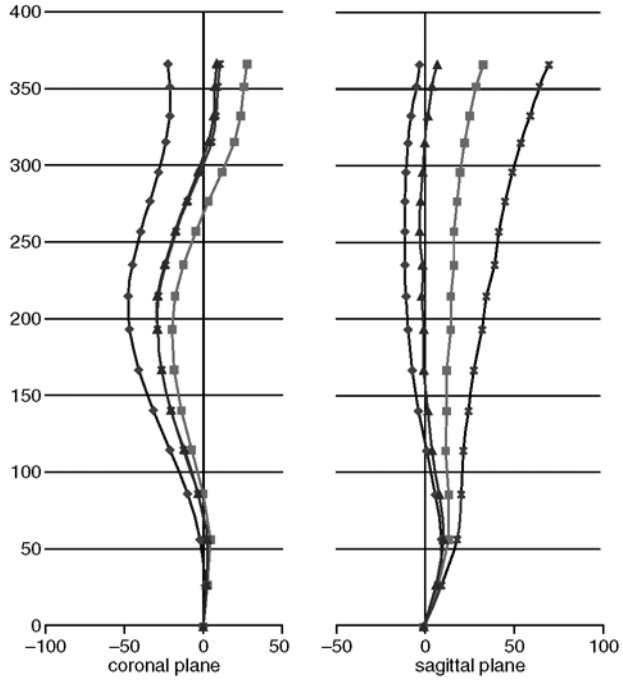

Fig. 5 *Spine curves of subject computed from FE model using different brace positioning from (–♦–) S1-T1, (–■–) L5, (–×–) pelvis transformation between in-brace and no-brace acquisitions, or (–▲–) with no positioning. All data are in mm*

Reaction forces were computed on the abdomen (47N), whereas negligible equivalent forces were measured.

The simulated geometry presented partially reduced coronal Cobb angles, more in the lumbar than in the thoracic zone, over-corrected sagittal Cobb angles and maximum deformation plane, completely corrected coronal shift, and sagittal shift and rib hump that were not corrected (Table 3). Fig. 4 illustrates the spine curves obtained in both the coronal and sagittal planes from the simulation and the no-brace and in-brace geometries.

The comparison between the different brace positions on the no-brace trunk model showed no changes in the Cobb angles. However, the coronal and sagittal shifts were modified owing to the different T1 positions found for each brace position (Fig. 5). The best agreement between the simulation and the in-brace geometry was obtained for the positioning using the pelvis transformation between the in-brace and the no-brace acquisitions.

4 Discussion and conclusions

An FE model of the brace and its interface with the torso and a refined model of the trunk were proposed to simulate the Boston brace treatment for a scoliotic spine. For one patient, the simulation results were compared with the geometry measured by a multiview radiographic technique (displacement validation) and with the pressure measured by a pressure matrix inserted at the brace–torso interface (force validation).

Some preliminary tests performed on the surface-to-surface contact element showed that the reaction forces were quite equivalent for a brace foam Young's modulus in the range of 10–5000 MPa, but were significantly reduced for a brace foam Young's modulus in the range of 0.1–1 MPa. The agreement between the reaction forces obtained from the simulations and the equivalent forces obtained from the pressure measurements justified the choice of the mechanical properties attributed to the brace–torso interface. The contact reaction forces computed in the sub-axillary and abdominal areas, but not calculated from the pressure analysis, could correspond to areas of low pressure neglected by the calculation of the equivalent forces (PÉRIÉ *et al.*, 2003). Only pressures higher than the clinically established pressure threshold of 30 mmHg (JIANG *et al.*, 1992) were used for the pressure areas delimitation and the computation of the equivalent forces.

The Cobb angles obtained from the simulations were partially corrected in the coronal plane, when compared with the real, in-brace correction. The reaction forces due to the contacts were not sufficient to achieve correction of thoracic scoliotic curves. This result suggested that other mechanisms such as muscle control to shift the trunk away from the pressure areas, could also participate in the correction of the scoliotic spinal curves, as suggested previously (PÉRIÉ *et al.*, 2003). This is compatible with recent findings of increased electromyography activity on the convex side of the lumbar curvatures, measured in the back muscles during Boston brace wearing (ODERMATT *et al.*, 2003). This result also suggested that the flexibility properties of the spine and rib cage, which were adapted from *ex vivo* experiments, did not adequately represent the real patient's flexibility. *In vivo* characterisation of patient-specific mechanical properties should be addressed in future investigations to improve the model.

As opposed to the coronal Cobb angle, the sagittal Cobb angles obtained from the simulations were over-aggravated, and the maximum deformation plane was overcorrected, when compared with the real, in-brace correction. These results suggested that muscle control contributes, not only to the spine curve correction in the coronal plane, but also to the prevention of back flattening in the sagittal plane and to global 3D correction of the curves. The transverse rib hump from the simulation was not corrected, as opposed to the real, in-brace measures, suggesting also that the flexibility properties of the rib cage and the costo-vertebral, costo-transverse and zygapophyseal joints may be too stiff.

The brace misalignment did not influence the spine curves, only the orientation of the L5-T1 axis. These results suggested that the errors made on the brace pad localisation have a minimum effect on the simulation results. An ideal simulation would rotate the brace during its closing to keep it aligned with the L5-T1 axis, or would let the brace be free to move instead of being fixed on the anterior side. However, in both cases, we will not be able to explain the changes observed on the T1 position by either a change in the patient's positioning or a righting reflex because of the brace.

The possible sources of error of the model concerned both the method used to analyse the measurements and the choices made for the simulation. The accuracy of the multiview radiographic reconstruction technique used for the acquisition of the personalised geometrical data was 3.3 ± 3.8 mm (DELORME *et al.*, 2003), but simulated errors of 5mm introduced in the model geometry did not influence the simulation results. The accuracy of the pressure transducers was ± 5 mmHg, and the method used to analyse the pressure neglected pressure less than 30 mmHg, according to JIANG *et al.* (1992). This limit could introduce the differences found between the reaction forces obtained in the contact elements and the equivalent forces calculated from the pressure measurements. The non-personalised mechanical properties attributed to the torso elements could influence the simulation results.

The specific structures that are critical to the trunk model and for which the data are especially poor are the intervertebral joint and the costo-vertebral, costo-transverse and zygapophyseal joints. Only the passive mechanisms were represented in this model. The results showed that the simulations induced only a partial correction when compared with the real, in-brace correction measured on the radiographs. We assumed that the remaining correction was attributable to the active mechanisms not represented in the model. A future study should incorporate a representation of the neuro-muscular control to complete the model and verify our assumption.

The FE model used in this study is considered to be an improvement over previous biomechanical models used for bracing simulations (ANDRIACCHI *et al.*, 1976; AUBIN *et al.*, 1995; GIGNAC *et al.*, 2000; PATWARDAN *et al.*, 1986; WYNARSKY and SCHULTZ, 1991), based on the following reasons. First, a personalised representation of the abdominal and thoracic soft tissue was integrated to represent more realistically the load transfer from the brace–torso interface to the spine and rib cage. Secondly, the FE model included, for the first time, an explicit representation of the brace and its interface with the torso. The 8-node brick elements and the surface-to-surface contact elements used for the brace and the brace–torso interface represent more adequately the complex 3D action of the brace on the torso than the models applying forces directly on the spine and rib-cage. These last 'force' models were limited by the small effect of the applied brace forces on the spine curve, and also by the important deformation created by the applied brace forces on the ribs, which suggested that the load transfer from the brace to the spine was not correctly represented (PÉRIÉ *et al.*, 2003).

The clinical relevance of these new modelling tools developed for the simulation of the brace treatment of scoliotic spine is the optimisation of the brace design for an improved treatment. In recent years, the manufacture of the brace has included computer techniques. The geometry of the brace is shaped directly on the screen instead of being cast on the patient. Then, the geometry files are sent to the manufacturer. An FE model that includes the brace representation would be useful for design of the brace and to verify its efficiency before its manufacture.

Acknowledgments—This study was funded by the Natural Sciences & Engineering Research Council of Canada, the Fond pour la formation de Chercheurs et d'Aide à la Recherche (Québec) and the Institut National de la Santé et de la Recherche Médicale (France). Part of the finite element model used in this study was developed in collaborative association with the Biomechanics Laboratory of the ENSAM (Paris, France; Drs F. Lavaste, W. Skalli and J.L. Descrimes).

References

ANDRIACCHI, T. P., SCHULTZ, A. B., BELYTSCHKO, T., and DEWALD, R. L. (1976): 'Milwaukee brace correction of idiopathic scoliosis', *J. Bone Joint Surg.*, **58A**, pp. 806–815

AUBIN, C. É., DANSEREAU, J., and LABELLE, H. (1993): 'Biomechanical simulation of the effect of the Boston brace on a model of the scoliotic spine and thorax (in French)', *Ann. Chir.*, **47**, pp. 881–887

AUBIN, C. E., DESCRIMES, J. L., DANSEREAU, J., SKALLI, W., LAVASTE, F., and LABELLE, H. (1995): 'Geometrical modeling of the spine and thorax for biomechanical analysis of scoliotic deformities using finite element method (in French)', *Ann. Chir.*, **49**, pp. 749–761

BISCHOFF, J. E., ARRUDA, E. M., and GROSH, K. (2000): 'Finite element modeling of human skin using an isotropic, nonlinear elastic constitutive model', *J. Biomech.*, **33**, pp. 645–652

DANSEREAU, J., CÔTÉ, B., LABELLE, H., and AUBIN, C.-É. (1992): 'Measurement of forces generated by Boston brace in the treatment of scoliotic deformities', *J. Biomech.*, **25**, p. 656

DELORME, S., PETIT, Y., DE GUISE, J., LABELLE, H., AUBIN, C. É., and DANSEREAU, J. (2003): 'Assessment of the 3D reconstruction and high-resolution geometrical modeling of the human skeletal trunk from 2D radiograhic images', *IEEE Tr. Biomed. Eng.*, **50**, pp. 989–998

DESCRIMES, J. L., AUBIN, C. É., SKALLI, W., ZELLER, R., DANSEREAU, J., and LAVASTE, F. (1995): 'Introduction des facettes articulaires dans une modélisation par éléments finis de la colonne vertébrale et du thorax scoliotique: aspects mécaniques', *Rachis*, **7**, pp. 301–314

DIETRICH, M., HEDZIOR, K., and ZAGRAJEK, T. (1991): 'A biomechanical model of the human spinal system', *Proc. Instn. Mech. Eng.*, **205**, pp. 19–26

GIGNAC, D., AUBIN, C. E., DANSEREAU, J., and LABELLE, H. (2000): 'Optimization method for 3-D bracing correction of scoliosis using a finite element model', *Eur. Spine J.*, **9**, pp. 185–190

JIANG, H., RASO, W., HILL, D., DURDLE, N., and MOREAU, M. (1992): 'Interface pressure in the Boston brace treatment for scoliosis: a preliminary study'. Int. Symposium on 3D Scoliotic Deformities (Editions de l'Ecole Polytechnique, Montréal, and Gustav Fischer Verlag, Stuttgart), pp. 395–399

LABELLE, H., DANSEREAU, J., BELLEFLEUR, C., and POITRAS, B. (1996): 'Three-dimensional effect of the Boston brace on the thoracic spine and the rib cage', *Spine*, **21**, pp. 59–64

MAC-THIONG, J. M., PETIT, Y., DELORME, S., DANSEREAU, J., AUBIN, C. É., and LABELLE, H. (2004): 'Biomechanical evaluation of the Boston brace for the treatment of AIS: relationship between strap tension and brace pressure interface', *Spine*, **29**, pp. 26–32

MARRAS, W. S., and SOMMERICH, C. M. (1991): 'A three-dimensional motion model of loads on the lumbar spine: I. Model structure', *Hum. Factors*, **33**, pp. 123–137

ODERMATT, D., MATHIEU, P. A., BEAUSÉJOUR, M., LABELLE, H., and AUBIN, C. E. (2003): 'Electromyographic study of adolescent idiopathic scoliosis patients treated with the Boston brace', *J. Orthop. Res.*, **21**, pp. 931–936

OGILVIE, J. (1994): WEINSTEIN, S. L. (Ed.): 'Spinal orthotics. An Overview, the Pediatric Spine: Principles and Practice' (Raven Press Ltd., New York, USA, 1994), pp. 1787–1793

PATWARDAN, A. G., BUNCH, W. H., MEADE, K. P., VANDERBY, R. J., and KNIGHT, G. W. (1986): 'A biomechanical analog of curve progression and orthotic stabilization in idiopathic scoliosis', *J. Biomech.*, **19**, pp. 103–117

PÉRIÉ, D., SALES DE GAUZY, J., and HOBATHO, M. C. (2002): 'Biomechanical evaluation of Cheneau–Toulouse–Munster brace in the treatment of scoliosis using optimisation approach and finite element method', *Med. Biol. Eng. Comput.*, **40**, pp. 296–301

PÉRIÉ, D., AUBIN, C. E., PETIT, Y., BEAUSÉJOUR, M., DANSEREAU, J., and LABELLE, H. (2003): 'Boston brace correction in idiopathic scoliosis: A biomechanical study', *Spine*, **28**, pp. 1672–1677

PETIT, Y., AUBIN, C. E., DANSEREAU, J., GIGNAC, D., JONCAS, J., DE GUISE, J. A., and LABELLE, H. (1998): 'Effect of strap tension on the pressure generated by the Boston brace on idiopathic scoliosis patients: a preliminary study', *J. Biomech.*, **31**, p. 175

STOKES, I. A. (1994): 'Three-dimensional terminology of spinal deformity. A report presented to the Scoliosis Research Society by the Scoliosis Research Society. Working Group on 3-D terminology of spinal deformity', *Spine*, **15**, pp. 236–248

SUNDARAM, S. H., and FENG, C. C. (1977): 'Finite element analysis of the human thorax', *J. Biomech.*, **10**, pp. 505–516

UEYOSHI, A., and SHIMA, Y. (1985): 'Studies on spinal braces, with special reference to the effects on increased abdominal pressure', *Int. Orthop.*, **9**, pp. 255–258

WYNARSKY, G. T., and SCHULTZ, A. B. (1991): 'Optimization of skeletal configuration: studies of scoliosis correction biomechanics', *J. Biomech.*, **24**, pp. 721–732

Author's biography

DELPHINE PÉRIÉ received the PhD in mechanical engineering (biomechanics) from University Paul Sabatier, Toulouse, France, in 1999. After two years as a Postdoctoral Fellow at Queen's University, Kingston, Canada and Hospital Ste Justine, Montreal, Canada, she held an Assistant Professor position for two years in the Sport Sciences department, University Paul Sabatier. Since January 2003, she has been working as a Research Associate in the Mechanical Engineering department, University of Vermont, USA. Her research activities concerned the biomechanical characterization and modelling of the musculo-skeletal system, with a main interest in the *in vivo* study of the biomechanical behaviour of soft tissues using medical imaging.